British Journal of Pharmacology (1995) 116, 1729-1736

[^{3}H]-RS-45041-190: a selective high-affinity radioligand for I_2 imidazoline receptors

Alison C. MacKinnon, [2]William S. Redfern & [1,2]Christine M. Brown

Department of Pharmacology, Syntex Research Centre, Research Park, Riccarton, Edinburgh EH14 4AP

1 RS-45041-190 (4-chloro-2-(imidazolin-2-yl)isoindoline) is an I_2 imidazoline receptor ligand with the highest affinity and selectivity so far described; [^{3}H]-RS-45041-190 has a tritium atom attached to the 7-position on the isoindoline ring.

2 [^{3}H]-RS-45041-190 binding to rat kidney membranes was saturable ($B_{max} = 223.1 \pm 18.4$ fmol mg^{-1} protein) and of high affinity ($K_d = 2.71 \pm 0.59$ nM). Kinetic studies revealed that the binding was rapid and reversible, with [^{3}H]-RS-45041-190 interacting with two sites or two affinity states.

3 Competition studies showed that 60-70% of [^{3}H]-RS-45041-190 binding (1 nM) was specifically to imidazoline binding sites of the I_2 subtype, characterized by high affinity for idazoxan (pIC_{50} 7.85 ± 0.03) and cirazoline (pIC_{50} 8.16 ± 0.05). The remaining 30-40% was displaced specifically by the monoamine oxidase A inhibitors, clorgyline and pargyline.

4 α_1- and α_2-adrenoceptor, I_1 imidazoline, histamine, 5-hydroxytryptamine or dopamine receptor ligands had low affinity suggesting that [^{3}H]-RS-45041-190 did not label receptors of these classes.

5 In autoradiography studies, [^{3}H]-RS-45041-190 labelled discrete regions of rat brain corresponding to the distribution of I_2 subtypes, notably the subfornical organ, arcuate nucleus, interpeduncular nucleus, medial habenular nucleus and lateral mammillary nucleus, and additional sites in the locus coeruleus, dorsal raphe and dorsomedial hypothalamic nucleus.

6 [^{3}H]-RS-45041-190 therefore labels I_2 receptors with high affinity, and an additional site which has high affinity for some monoamine oxidase inhibitors.

Keywords: [^{3}H]-RS-45041-190; imidazoline receptors; I_2-selective; rat kidney

Introduction

The imidazoline radioligands [^{3}H]-*p*-aminoclonidine, [^{3}H]-clonidine and [^{3}H]-idazoxan, in addition to labelling α_2-adrenoceptors, also label populations of non-adrenoceptor binding sites. Imidazoline binding sites labelled with [^{3}H]-*p*-aminoclonidine in bovine ventrolateral medulla (Ernsberger *et al.*, 1987) and with [^{3}H]-clonidine in human brainstem (Bricca *et al.*, 1989) show high affinity for clonidine, rilmenidine and oxymetazoline and low affinity for the catecholamines noradrenaline and adrenaline, and have been termed I_1 (Ernsberger, 1992). The imidazoline binding sites labelled with [^{3}H]-idazoxan in a variety of tissues and species show high affinity for guanido-compounds and amiloride, moderate affinity for clonidine and low affinity for catecholamines and yohimbine (Hamilton *et al.*, 1988; MacKinnon *et al.*, 1989; Coupry *et al.*, 1989; Yablonsky & Dausse, 1989), and have been termed I_2 (Ernsberger, 1992).

In a search for an endogenous ligand for the imidazoline binding site(s), Atlas & Burnstein (1984) isolated and partially purified an extract from bovine brain which displaced [^{3}H]-clonidine from bovine cerebral cortex membranes. This endogenous clonidine displacing substance (CDS) was not a catecholamine but the exact chemical nature of its active constituent(s) was not established. Recently, however, analysis of a CDS extract also from bovine brain has suggested that the activity of CDS could be due to the presence of agmatine, a precursor of putrescine and other polyamines, and that agmatine could be the endogenous ligand for imidazoline receptors (Li *et al.*, 1994).

Up until now, characterization of imidazoline receptors has been limited, as currently-available imidazoline radioligands are relatively non-selective and have high affinity for α_2-adrenoceptors and other receptors. Therefore, the inclusion of specific blockers has been necessary to study the imidazoline binding site(s) in isolation (MacKinnon *et al.*, 1993). Recently, new radioligands for I_2 imidazoline receptors have been described, such as 2-[3-azido-4-[^{125}I]-iodophenoxy]methyl imidazoline ([^{125}I]-AZIPI; Lanier *et al.*, 1993) and [^{3}H]-2-(2-benzofuranyl-)-2-imidazoline ([^{3}H]-2-BFI; Lione *et al.*, 1995). The present paper describes the binding characteristics of [^{3}H]-4-chloro-2-(imidazolin-2-yl)isoindoline ([^{3}H]-RS-45041-190; Figure 1) a selective, high-affinity I_2 imidazoline radioligand which has low affinity for α_2-adrenoceptors and a variety of other receptors subtypes. We also describe the neuroanatomical distribution of its binding sites in the rat brain, studied by quantitative autoradiography.

A preliminary account of part of this work has been presented to the British Pharmacological Society (MacKinnon *et al.*, 1995).

Methods

Membrane preparation

Rat kidney membranes were prepared as previously described (MacKinnon *et al.*, 1993). Male Sprague-Dawley rats, 200-250 g, were killed by cervical dislocation and the kidneys re-

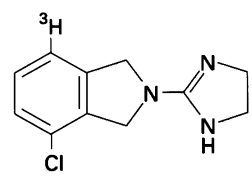

Figure 1 Structure of [^{3}H]-4-chloro-2-(imidazolin-2-yl) isoindoline ([^{3}H]-RS-45041-190).

[1] Author for correspondence.
[2] Present address: Quintiles Scotland Ltd, Research Park, Riccarton, Edinburgh EH14 4AP.

moved. Kidneys were homogenized in 25 volumes (w/v) 50 mM Tris HCl pH 8.0 at 4°C containing 5 mM EDTA with a Polytron PT 10 tissue disruptor. The homogenate was centrifuged at 48000 *g* for 15 min at 4°C. The supernatant was discarded and the pellet resuspended in the original volume of homogenizing buffer and recentrifuged. The pellet was washed twice by centrifugation in 50 mM Tris HCl (pH 8.0) at 4°C containing 0.5 mM EDTA, and the final pellet resuspended in 3 ml 50 mM Tris HCl (pH 8.0) at 4°C and stored under liquid N_2 until used in the binding assay.

Binding assays

[^{3}H]-RS-45041-190 was synthesized to a specific activity of 28 Ci mmol^{-1} by Dr H. Parnes (Institute of Chemistry, Syntex Palo Alto, U.S.A.), and stored at −20°C at a concentration of 1 mCi ml^{-1}. Under these storage conditions [^{3}H]-RS-45041-190 retained >96% purity (determined by h.p.l.c.) throughout the duration of this study. In saturation experiments, 0.2–25 nM [^{3}H]-RS-45041-190 was incubated with rat kidney membranes (200–400 μg protein) to equilibrium (60 min at 25°C) in an assay volume (500 μl) of 50 mM Tris HCl pH 7.4 at 25°C containing 0.5 mM EDTA. In competition experiments 1.0 nM [^{3}H]-RS-45041-190 was incubated with 13 concentrations of competing drug. Non-specific binding was defined in the presence of 10 μM cirazoline. Bound ligand was separated from free by filtration over Whatman GF/B filters in a Brandel Cell Harvester.

Autoradiography

Male Sprague-Dawley rats were anaesthetized with pentobarbitone and perfused intracardially with 20 ml 0.9% saline. The brains were removed and frozen in isopentane at −45°C, frozen onto microtome chucks and 20 μm coronal sections (in the plane of the atlas of Paxinos & Watson, 1986) thaw mounted onto gelatin subbed slides. Frozen sections were stored at −20°C for 3 days before use. Sections were brought to room temperature and preincubated for 20 min at room temperature in Tris HCl buffer pH 7.4 containing 0.5 mM EDTA. Incubations were performed in the same buffer containing 8 nM [^{3}H]-RS-45041-190 for 60 min. Non-specific binding was determined in the presence of 10 μM cirazoline. Labelled sections were washed in ice cold Tris EDTA buffer for 10 min, dipped in ice cold distilled H_2O and dried in a stream of cold air. The sections were opposed to ^{3}H-sensitive Hyperfilm (Amersham) with appropriate standards (^{3}H microscales Amersham) for 6 weeks. Autoradiograms were quantified by a Quantimet 970 image analyser, and the atlas of Paxinos & Watson (1986) was used to identify structures.

Data analysis

Binding isotherms from competition studies were analysed by a non-linear least squares curve fitting programme capable of fitting to a one- or two-site model. The IC_{50} (concentration of drug displacing 50% specific binding) was converted to the inhibitory constant (K_i) by the equation of Cheng & Prusoff (1973) where $K_i = IC_{50}/(1 + [\text{ligand}]/K_d)$. The fits for a one- and two-site model were compared using the differential F value. A two-site fit was assumed to be significantly better than a one-site fit if the determined F value had a $P<0.05$. Equilibrium binding parameters (K_d and B_{max}) were obtained by the iterative non-linear least squares curve fitting programme, LIGAND (Munson & Rodbard, 1980).

For kinetic experiments, the pseudo first order rate constant (K_{obs}) was calculated from a non-linear squares fit to a single exponential function (Eq.1), using the KaleidaGraph programme run on an Apple Macintosh computer, where Be and k are, respectively, the amount of equilibrium binding and the rate constant (K_{obs}) for the single exponential model, and Bt is the binding at time t. Experiments were also analysed according to a double exponential fit (Eq.2), where Be_f and Be_s are the amplitudes, and k_f and k_s are the rates

$$Bt = Be\,(1 - e^{-k}) \quad \text{(Eq.1)}$$

$$Bt = Be_F\,(1 - e^{-k_F}) + Be_s(1 - e^{-k_s}) \quad \text{(Eq.2)}$$

(K_{obs}) of the fast and slow binding components in the double exponential model. The fits for a one or two site model were compared using the differential F value (see above). The association rate constant K_1, was determined from the equation $K_1 = (K_{obs} - K_2)/[\text{ligand}]$, where K_2 is the dissociation rate constant calculated from a non-linear least-squares fit to a single or double exponential function (Eq.3 and 4) where B0 represents binding at time 0.

$$Bt = B0\,(-e^{-k}) \quad \text{(Eq.3)}$$

$$Bt = B0_F(-e^{-k_F}) + B0_s(-e^{-k_s}) \quad \text{(Eq.4)}$$

The equilibrium dissociation constant (K_d) was calculated from the equation $K_d = K_2/K_1$.

Chemicals and drugs

Reagents and chemicals used were of the highest analytical grade available. Compounds were kindly donated by their manufactureres, synthesized at the Institute of Organic Chemistry, Syntex (Palo Alto) or purchased. The following compounds were used: (–)-adrenaline bitartrate, pargyline HCl, amiloride HCl, histamine HCl, dopamine HCl, GppNHp, agmatine HCl and naphazoline HCl (Sigma); *p*-aminoclonidine HCl, clorgyline HCl and selegiline HCl (Research Biochemicals Incorporated); cirazoline HCl (Synthelabo); guanabenz (Wyeth); prazosin HCl (Pfizer); delequamine HCl (RS-15385-197), RS-45041-190 (4-chloro-2-(imidazolin-2-yl)isoindoline), rilmenidine and idazoxan HCl were synthesized by Dr R. Clark, Syntex Palo Alto, U.S.A.

Results

[^{3}H]-RS-45041-190 binding to rat kidney

Kinetics [^{3}H]-RS-45041-190 binding to rat kidney membranes was rapid and reversible (Figure 2). Equilibrium was reached within 60 min, but the time course of [^{3}H]-RS-45041-190 binding was better fitted to two exponential phases of binding. The rate constant K_{obs} for the fast phase of binding was 1.395 ± 0.518 min^{-1} with $t_{1/2}$ = 35 s and represented 53 ± 6% of the total bound ligand at equilibrium. The remaining binding associated slowly (K_{obs} = 0.055 ± 0.035 min^{-1} with $t_{1/2}$ = 12.6 min; n = 4 in each case). After the addition of 10 μM cirazoline, [^{3}H]-RS-45041-190 exhibited a biphasic dissociation plot with 57 ± 6% dissociating rapidly (K_2 = 0.401 ± 0.118 min^{-1}, $t_{1/2}$ = 1.7 min). The remaining binding dissociated slowly (K_2 = 0.037 ± 0.010 min^{-1}, $t_{1/2}$ = 19 min). K_d values were calculated based on the percentage of rapidly associating and dissociating components, thus, K_d values of 0.57 ± 0.21 nM for the fast phase and 0.89 ± 0.15 nM for the slow phase were obtained. These results indicated that [^{3}H]-RS-45041-190 labelled two sites or two affinity states of an imidazoline binding site on rat kidney.

Saturation analysis [^{3}H]-RS-45041-190 binding was of high affinity and saturable in the rat kidney (Figure 3). The data were better fitted to a one-site model (K_d = 2.71 ± 0.59 nM, B_{max} = 223.1 ± 18.4 fmol mg^{-1} protein; n = 6). At the K_d concentration, the percentage of binding defined with 10 μM cirazoline was 70–75% of the total [^{3}H]-RS-45041-190 bound. The failure of saturation analysis to define two sites for [^{3}H]-RS-45041-190 was probably due to the very similar affinity shown for the two sites in kinetic experiments (see previous section).

Competition studies In competition experiments (Table 1), unlabelled RS-45041-190 showed high affinity (pK_i = 8.39) and a Hill slope of 0.75, suggesting that more than one site was being labelled with [^{3}H]-RS-45041-190. However, statistical analysis of the fits revealed that the data were not significantly better fitted to a two-site model (Figure 4). The imidazoline compounds idazoxan (Figure 4) and cirazoline displaced [^{3}H]-RS-45041-190 binding with high and low affinity components (pIC_{50} = 7.85 and 5.80 for idazoxan and 8.16 and 6.11 for cirazoline). The high affinity component represented 60–70% of the specifically bound [^{3}H]-RS-45041-190 (1 nM). The monoamine oxidase A inhibitors clorgyline and pargyline, but not the monoamine oxidase B inhibitor, selegiline, displaced 30–40% of the binding with high affinity (Figure 5, Table 1). Naphazoline inhibited [^{3}H]-RS-45041-190 binding with moderate affinity and a shallow Hill slope, although again this was not significantly better fitted to a two-site model. Guanabenz showed high affinity for [^{3}H]-RS-45041-190 binding and *p*-aminoclonidine showed very low affinity. These data suggest that 60–70% of the sites labelled with [^{3}H]-RS-45041-190 show characteristics of the I_2 imidazoline site. Other compounds tested (adrenaline, delequamine (RS-15385-197), dopamine, histamine, prazosin, rilmenidine and agmatine) had very low affinity for [^{3}H]-RS-45041-190 binding (pK_i < 5.6).

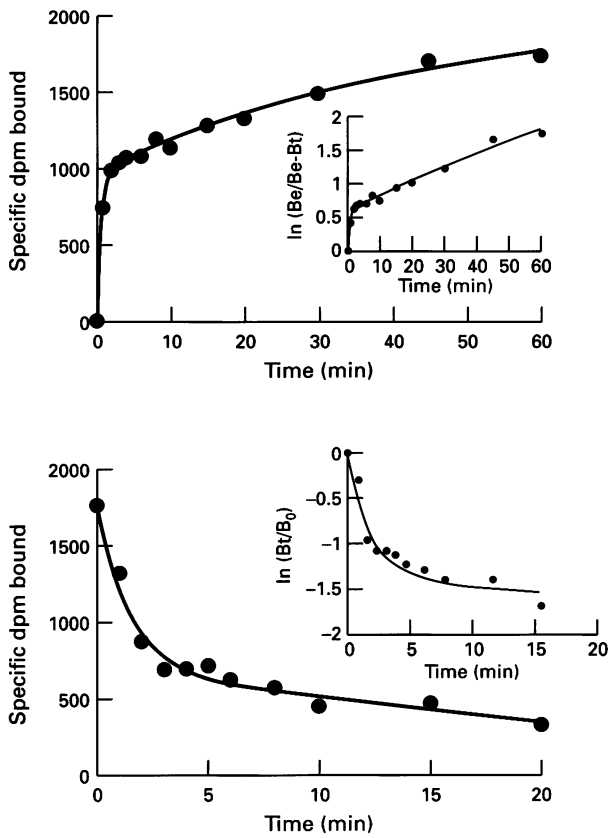

Figure 2 Association and dissociation of [^{3}H]-RS-45041-190 binding to rat kidney membranes. The inserts show the semilogarithmic plots of the data. The data represent a single experiment performed in triplicate. Essentially similar data were obtained in three other experiments on different preparations (see text for mean values). Two association rate constants (top panel) were calculated: K_{obs1} = 1.376, K_{obs2} = 0.0346 min^{-1}. On the addition of 10 μM cirazoline, [^{3}H]-RS-45041-190 dissociated with two rate constants: K_{21} = 0.714, K_{22} = 0.0204 min^{-1}. Calculated K_d values for the fast and slow components were 1.18 and 1.57 nM respectively.

Effect of 5'guanylylimidodiphosphate (Gpp(NH)p) on [^{3}H]-RS-45041-190 binding In order to determine whether the [^{3}H]-RS-45041-190 binding site(s) couple to a G-protein, the

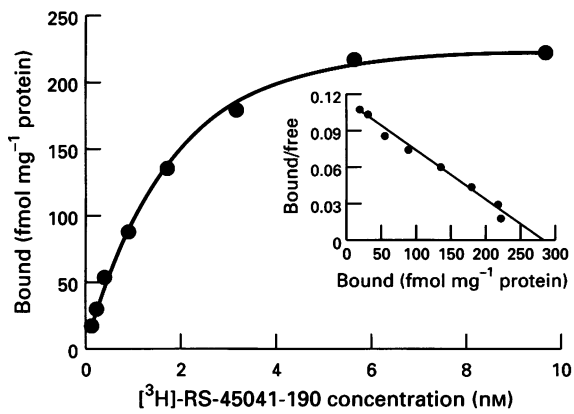

Figure 3 Saturation analysis of [^{3}H]-RS-45041-190 binding to rat kidney membranes. The data represent a typical experiment performed in triplicate. Essentially similar data were obtained in five other experiments on different preparations (see text for mean values). The insert shows the Scatchard plot of the data. The affinity (K_d) = 1.91 nM and the B_{max} = 280.1 fmol mg^{-1} protein.

Table 1 Inhibition of [^{3}H]-RS-45041-190 binding in rat kidney membranes

Compound	n	pK_i	*nH*	pIC_{50} (60–70%)	pIC_{50} (30–40%)
RS-45041-190	3	8.39 ± 0.04	0.75 ± 0.02		
Idazoxan	3			7.85 ± 0.03	5.80 ± 0.12
Cirazoline	3			8.16 ± 0.05	6.11 ± 0.17
Clorgyline	3			5.65 ± 0.20	8.60 ± 0.27
Pargyline	3			4.43 ± 0.71	7.76 ± 0.54
Selegiline	3	5.25 ± 0.20	0.69 ± 0.02		
Guanabenz	3	7.23 ± 0.07	1.23 ± 0.10		
Amiloride	3	6.91 ± 0.36	0.72 ± 0.03		
Naphazoline	4	6.61 ± 0.11	0.62 ± 0.02		
Rilmenidine	3	5.57 ± 0.18	0.61 ± 0.07		
p-Aminoclonidine	3	4.89 ± 0.15	0.77 ± 0.08		
Agmatine	3	< 4			
Adrenaline	3	< 4			
Delequamine	3	< 4	–		
Dopamine	2	5.08	0.72		
Histamine	2	4.13	–		
Prazosin	2	4.20	–		

A range of concentrations of inhibitor were incubated with 1 nM [^{3}H]-RS-45041-190 and rat kidney membranes to equilibrium as described in Methods. The results represent the mean ± s.e.mean of *n* determinations performed in duplicate. For compounds displaying biphasic displacement curves the pIC_{50} and % binding of each component is given.

regulation of binding by Gpp(NH)p was determined. Gpp(NH)p did not compete for [^{3}H]-RS-45041-190 binding at concentrations up to 1 mM (data not shown). However, for G-protein-coupled receptors, guanylnucleotides change the affinity state of the receptor for its agonist to a low affinity state. One potential agonist is idazoxan, as it gave rise to a biphasic inhibition curve in competition experiments; therefore inhibition curves to idazoxan were carried out in the presence and absence of 100 μM Gpp(NH)p. Figure 4 shows that the affinity and the percentage of sites defined with idazoxan were unaltered by the presence of 100 μM Gpp(NH)p (control: $pIC_{50} = 7.74 \pm 0.03$ (69%) and 5.75 ± 0.18 (21%); 100 μM Gpp(NH)p: $pIC_{50} = 7.93 \pm 0.11$ (68%) and 5.56 ± 0.31 (22%), $n = 3$). These data suggest that either idazoxan is not an agonist or that the binding sites are not coupled to a G-protein.

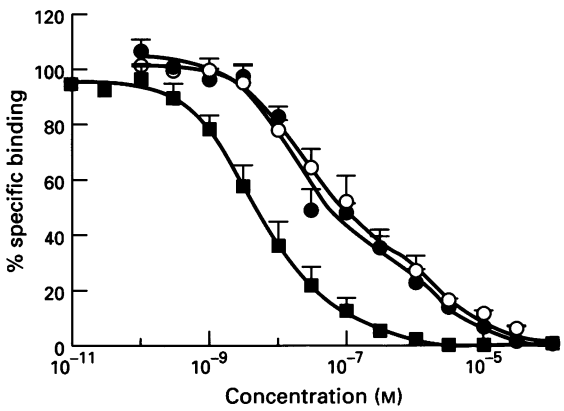

Figure 4 Effect of RS-45041-190 and idazoxan on [^{3}H]-RS-45041-190 binding in rat kidney: (●) idazoxan; (○) idazoxan plus GppNHp (100 μM); (■) RS-45041-190. The data represent the mean ± s.e.mean of three experiments on different preparations each performed in duplicate. For idazoxan the data were better fitted to a two-site model in the presence and absence of Gpp(NH)p. Affinity values as given in the text.

Autoradiographical distribution of imidazoline binding sites in rat brain

[^{3}H]-RS-45041-190 binding sites were highly localized in discrete regions of rat brain. Table 2 shows the density of binding sites measured in several regions of rat brain. Images of total

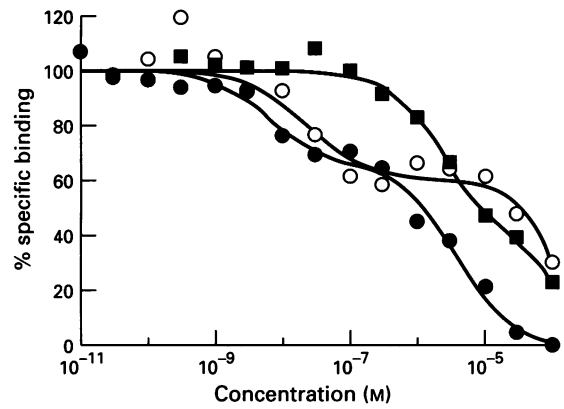

Figure 5 Effect of monoamine oxidase inhibitors on [^{3}H]-RS-45041-190 binding. The data represent a typical experiment performed in duplicate. Essentially similar data were obtained in three other experiments on different preparations (see text for mean values). For clorgyline (●) and pargyline (○) the data were better fitted to a two-site model with pIC_{50}s of 8.60 and 7.81 for the high affinity component (35%) and 5.83 and 4.41 for the low affinity component (65%), respectively. Selegiline (■) was better fitted to a one-site model with a low Hill slope ($pIC_{50} = 5.27$, $n_H = 0.63$).

Table 2 Distribution of [^{3}H]-RS-45041-190 binding in rat brain

Region	*Specific binding* (fmol mg^{-1} tissue)	*Region*	*Specific binding* (fmol mg^{-1} tissue)
Olfactory system		*Cortical regions*	
Ant. olfactory nuc. lat.	97.1 ± 10.6	entorhinal cortex	85.1 ± 8.2
Septal area		occipital cortex	62.6 ± 5.6
subfornical organ	195.7 ± 12.2	temporal cortex	62.7 ± 2.9
lateral ventricles	103.0 ± 6.4	parietal cortex	38.3 ± 2.0
Corpus striatum		cingulate cortex	43.3 ± 1.6
caudate putamen	52.1 ± 4.6	cor/amygdloid zone	124.5 ± 16.4
globus pallidus	11.1 ± 1.4	orbital cortex	88.5 ± 17.7
nuc. accumbens	101.3 ± 9.6	*Pons*	
Thalamic regions		locus coeruleus	184.5 ± 15.6
paraventricular	125.9 ± 3.1	olivocochlear bundle	110.9 ± 25.5
medial habenular nuc.	159.2 ± 9.4	ventrospinal cer. tract	86.4 ± 5.8
fasciculus retroflexus	88.7 ± 15.0	pontine nuclei	35.7 ± 4.8
Hypothalamic regions		dorsal tegmental nuc.	76.9 ± 3.4
dorsomedial	237.6 ± 29.7	dorsal raphe	135.1 ± 20.6
arcuate nuc.	247.3 ± 10.2	*Medulla*	
mammillary nuc. med.	152.9 ± 81.4	gracile nucleus	56.1 ± 12.9
mammillary peduncle	112.8 ± 16.2	hypoglossal nuc.	71.3 ± 8.3
Hippocampal regions		nuc. spin. tract trig.	9.7 ± 1.2
dentate gyrus	62.7 ± 5.7	area postrema	215.6 ± 25.8
subiculum	97.8 ± 16.5	lateral reticular nuc.	40.7 ± 4.1
CA1	105.4 ± 8.7	pyramidal tract	66.3 ± 10.5
CA2	97.6 ± 8.0	nuc. sol. tract	100.6 ± 5.7
CA3	89.2 ± 11.0	inferior olive	76.4 ± 3.1
Mesencephalon		paramedian lobule	35.4 ± 4.3
periaqueductal grey	93.4 ± 4.1	*Cerebellar regions*	
interpeduncular nuc.	217.4 ± 21.7	C1	57.9 ± 5.7
substantia nigra	32.9 ± 0.8	C9	24.1 ± 3.7

Sections were labelled with 8 nM [^{3}H]-RS-45041-190 as described in Methods. Quantification of image density in fmol mg^{-1} tissue was carried out with a Quantimet 970 image analyser. The results represent the mean ± s.e.mean of multiple measurements made from 3–4 animals.

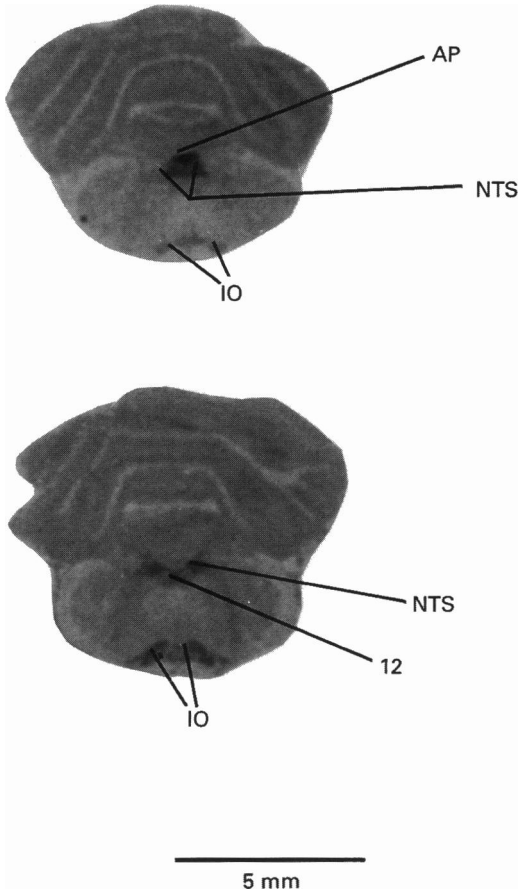

Figure 6 [^{3}H]-RS-45041-190 binding in rat brain (medullary region). The images show representative total binding sections through the rat brain. Non-specific binding in consecutive sections was not significantly greater than background. AP (area postrema), IO (inferior olive), NTS (nucleus of the solitary tract), 12 (hypoglossal nucleus).

binding sections are presented in Figures 6–8. High density binding (>150 fmol mg^{-1} tissue) was observed in the area postrema, the interpeduncular and the arcuate nuclei, lateral ventricles, subfornical organ, locus coeruleus, medial habenular nucleus and the dorsomedial hypothalamic nucleus, with moderate binding (100–150 fmol mg^{-1} tissue) in the olivocochlear bundle, dorsal raphe, cortical amygdaloid zone, periaqueductal grey and the nucleus of the solitary tract.

Discussion

[^{3}H]-RS-45041-190 was shown to be a selective I_2 imidazoline ligand which displayed high affinity for an imidazoline binding site on rat kidney membranes. Competition studies showed adrenaline and delequamine (RS-15385-197; Brown *et al.*, 1993) to have negligible affinity suggesting that this ligand does not label α_2-adrenoceptors. In addition, ligands for α_1-adrenoceptors, I_1, histamine, 5-HT and dopamine receptors had low affinity suggesting that [^{3}H]-RS-45041-190 did not label receptors of these classes. Kinetic analysis showed that [^{3}H]-RS-45041-190 labelled two sites in rat kidney (K_d=0.57 nM and 0.89 nM); however, in saturation studies and in competition experiments with unlabelled RS-45041-190 the data were better fitted to a one-site model. This could be explained by the lack of resolution in the latter two analyses given that the affinities calculated from kinetic experiments differed by less than twofold. Inhibition curves to idazoxan and cirazoline confirmed that [^{3}H]-RS-45041-190 labelled two sites as they showed >100-fold selectivity for 60–70% of the binding, and clorgyline and pargyline showed >1000-fold selectivity for the remainder of the binding.

A comparison was made of affinities of a range of compounds for [^{3}H]-RS-45041-190 binding in rat kidney (present study) and for [^{3}H]-idazoxan binding in this tissue (data from MacKinnon *et al.*, 1993) and in rat brain (data from Brown *et al.*, 1990). Figure 9 shows a very good correlation between [^{3}H]-RS-45041-190 binding in rat kidney and [^{3}H]-idazoxan binding in the same tissue (r=0.97, slope=0.97) and in rat brain (r=0.93, slope=0.96). This indicates that the major component labelled by [^{3}H]-RS-45041-190, *i.e.* that which has high affinity for idazoxan and cirazoline but low affinity for clorgyline and pargyline, was similar to the sites labelled by [^{3}H]-idazoxan in rat kidney and brain. [^{3}H]-RS-45041-190 therefore labels an imidazoline receptor of the I_2 subtype in rat kidney which appears to be similar to the I_2 subtype in rat brain. The proposed endogenous ligand for imidazoline receptors, agmatine, did not displace [^{3}H]-RS-45041-190 binding (pK_i<4). The reason for this is at present unclear; however, the role of this substance in imidazoline receptor pharmacology and the physiological role of these receptors remains to be elucidated.

The possibility that [^{3}H]-RS-45041-190 was labelling both states of a G protein-linked receptor exhibiting high and low affinity states for agonists was addressed in experiments with the stable GTP analogue, Gpp(NH)p. Idazoxan exhibited a biphasic inhibition curve against [^{3}H]-RS-45041-190, and for that reason represented a likely candidate for an agonist at the imidazoline site. However, 100 μM Gpp(NH)p had no effect on the affinity or the percentage of sites defined with idazoxan suggesting that either idazoxan is not an agonist or that [^{3}H]-RS-45041-190 binding sites are not associated with a G-protein.

The distribution of binding sites labelled by [^{3}H]-RS-45041-190 in rat brain autoradiography studies showed some overlap

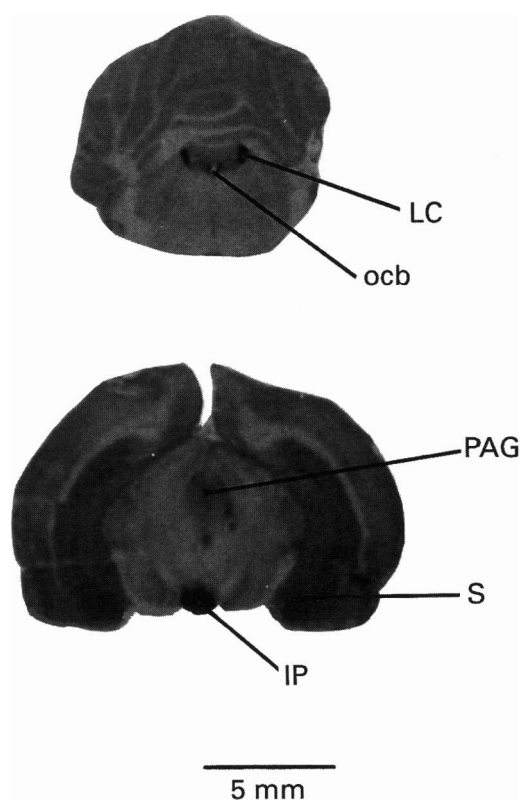

Figure 7 [^{3}H]-RS-45041-190 binding in rat brain (pons-midbrain region). The images show representative total binding sections through the rat brain. Non-specific binding in consecutive sections was not significantly greater than background. PAG (periaqueductal grey), IP (interpeduncular nucleus), LC (locus coeruleus), ocb (olivocochlear bundle), S (subiculum).

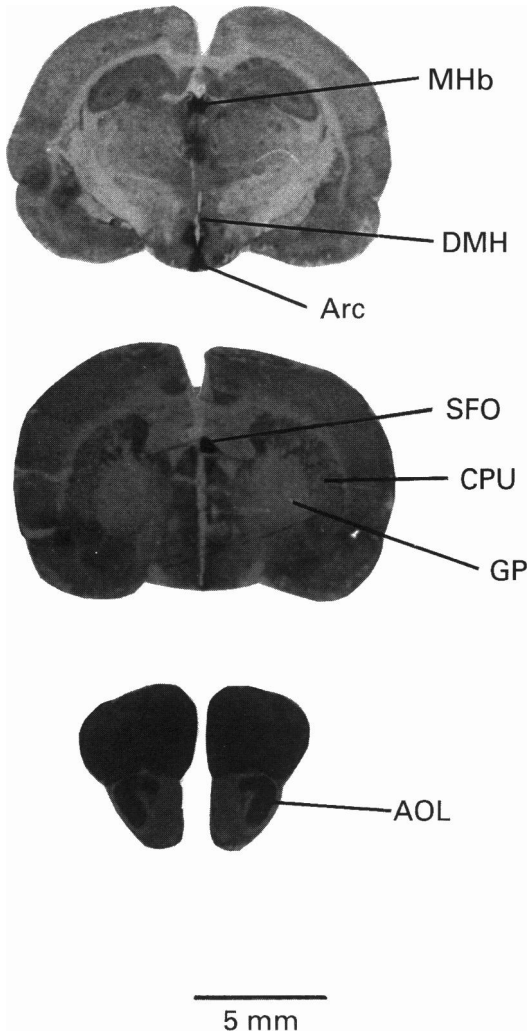

Figure 8 [^{3}H]-RS-45041-190 binding in rat brain (forebrain region). The images show representative total binding sections through the rat brain. Non-specific binding in consecutive sections was not significantly greater than background. Arc (arcuate nucleus), AOL (anterior olfactory nucleus, lateral), CPu (caudate putamen), DM-(dorsomedial hypothalamic nucleus), GP (globus pallidus, LM (lateral mammillary nucleus), MHb (medial habenular nucleus), SFO (subfornical organ).

with the distribution of I_2 receptors labelled by [^{3}H]-idazoxan (Mallard *et al.*, 1992; MacKinnon *et al.*, 1992). The binding sites for both ligands showed a very discrete neuroanatomical distribution, including the subfornical organ, arcuate nucleus, interpenduncular nucleus, lateral mammillary nucleus, medial habenula, nucleus tractus solitarius and area postrema. In addition to labelling those regions labelled by [^{3}H]-idazoxan, [^{3}H]-RS-45041-190 also labelled other discrete nuclei, including the dorsomedial hypothalamic nucleus, dorsal raphe nucleus, locus coeruleus and inferior olive. However, it should be pointed out that in neither study can we know whether the binding sites are neuronal.

The arcuate nucleus is associated with pituitary functions in particular, and a large number of hormones and peptides are found here (Chronwall, 1985). A recent study from this laboratory (MacKinnon *et al.*, 1992) investigated the affinity of many of these substances for I_2 sites in rabbit renal cortex, using displacement of [^{3}H]-idazoxan in the presence of dequamine. ACTH and LH showed moderate affinity ($pK_i = 5.86$ and 5.80, respectively). All other substances showed $pK_i < 5$, *viz.* LHRH, GHRH, angiotensin I and II, progesterone, testosterone, β-oestradiol, endothelin (ET-1), ADH, FMRF-NH_2, prolactin, dynorphin, neuropeptide Y, somatostatin, acetylcholine, GABA, substance P, TRH, Met-enkephalin, Met-enkephalinamide, oxytocin, VIP, α-MSH, γ-MSH, neurotensin, galanin, gastrin, renin and β endorphin. Thus, none of these endogenous ligands are likely to have activity at I_2 receptors.

It is interesting that the arcuate nucleus has direct axonal projections to many of the other nuclei highlighted in the present study, including the medial habenular nucleus, dorsal raphe nucleus, locus coeruleus and nucleus tractus solitarius (Sim & Joseph, 1991), and also provides input (presumably indirectly) to neurones in the subfornical organ (Rosas-Arrelano *et al.*, 1993). The medial habenula in turn is connected to the interpeduncular nucleus by the habenulo-interpeduncular tract (Kataoka *et al.*, 1973). It is therefore possible that all these regions labelled by [^{3}H]-RS-45041-190 perform some integrated functions together. The effects of RS-45041-190 on some of the more prominent functions of these regions forms the basis of another study (Brown *et al.*, 1995).

No neurotransmitter, receptor or enzyme appears to have a distribution identical to that of the binding sites for [^{3}H]-RS-45041-190, but some closely resemble it. For example, angiotensin II receptors have a distribution in the CNS which overlaps with some of the areas, with AT_1 receptors predominantly located in the subfornical organ, nucleus tractus solitarius and area postrema, and AT_2 receptors in the inferior olive and locus coeruleus (Gehlert *et al.*, 1991; Song *et al.*,

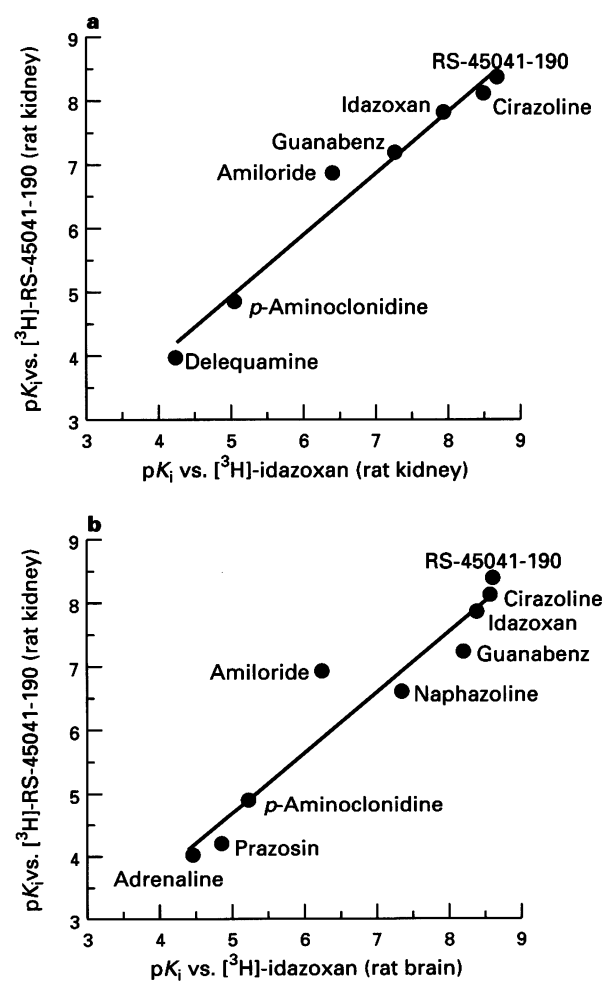

Figure 9 Correlation of binding affinities (pK_i) of several compounds for [^{3}H]-RS-45041-190 in rat kidney membranes (data from Table 1; data for idazoxan and cirazoline are the high-affinity pIC_{50} values) versus [^{3}H]-idazoxan binding in (a) rat kidney membranes ($r = 0.97$, slope = 0.97; data from MacKinnon *et al.*, 1993) and (b) rat brain membranes ($r = 0.93$, slope = 0.96; data from Brown *et al.*, 1990; RS-45041-190 rat brain pK_i value from Brown *et al.* (1995).

1992). However, as stated above, neither angiotensin I or II have appreciable affinity for imidazoline sites labelled with [^{3}H]-idazoxan, and it is therefore unlikely that imidazoline sites are associated with angiotensin II receptors in these areas. Enkephalins are also highly localized in the nucleus tractus solitarius, interpeduncular nucleus, arcuate nucleus and locus coeruleus (Zamir *et al.*, 1985), but as stated above, Met-enkephalin has no appreciable affinity for imidazoline sites defined by displacement of [^{3}H]-idazoxan binding in rabbit kidney. [^{3}H]-dexamethasone (which binds to glucocorticoid receptors) also shows high density binding in the arcuate nucleus, subfornical organ, locus coeruleus, nucleus tractus solitarius and area postrema (Birmingham *et al.*, 1993); interactions of glucocorticoids with the I_2 imidazoline site have not been investigated. Autoradiography studies with the MAO-A inhibitor, [^{3}H]-Ro 41-1049, have shown high levels of binding in the locus coeruleus, medial habenular and interpeduncular nuclei, nucleus tractus solitarius and inferior olives, whereas the distribution of MAO-B using the selective inhibitor, [^{3}H]-Ro 19- 6237, have shown the highest density of binding in the circumventricular organs (which include the subfornical organ and area postrema), the pineal gland and the arcuate nucleus (Saura *et al.*, 1992). Thus the distribution of MAO showed some striking parallels to the distribution of [^{3}H]-RS-45041-190 binding. It is tempting to suggest that the additional sites labelled by [^{3}H]-RS-45041-190 which are not labelled by [^{3}H]-idazoxan may represent binding to MAO-A, as they are sensitive to clorgyline and pargyline and show a similar distribution in rat brain. Alternatively, this secondary component of [^{3}H]-RS-45041-190 binding, which is sensitive to some MAO inhibitors, may represent an additional state or subclass of the I_2 receptor. Whatever the explanation, previous studies have shown that chronic treatment with clorgyline and phenelzine down-regulates I_2 binding sites in rat brain (Olmos *et al.*, 1993; Alemany *et al.*, 1995), suggesting a close association of the MAO enzyme complex and I_2 imidazoline receptors. It would also be interesting to investigate the interactions of the endogenous MAO inhibitor, isatin, with I_2 receptors. Isatin (indole-2,3-dione), a major consituent of the endogenous MAO inhibitor, tribulin (Glover *et al.*, 1988), is structurally similar to the isoindoline moeity of RS-45041-190 and could conceivably be an endogenous ligand for I_2 receptors.

This study has demonstrated that the imidazoline compound [^{3}H]-RS-45041-190 has a high affinity and selectivity for I_2 imidazoline receptors in rat kidney and brain and has low affinity for α_2-adrenoceptors and a variety of other receptors. It therefore represents a superior radioligand for use in the classification of imidazoline receptors, and for investigating their distribution in tissues by autoradiographic techniques.

[^{3}H]-RS-45041-190 was synthesized by Dr Howard Parnes, Syntex, Palo Alto, California, U.S.A. We thank Mr Charles Calder for printing the autoradiograms.

References

ALEMANY, R., OLMOS, G. & GARCIA-SEVILLA, J.A. (1995). The effects of phenelzine and other monoamine oxidase inhibitor antidepressants on brain and liver I_2 imidazoline-preferring receptors. *Br. J. Pharmacol.*, **114,** 837–845.

ATLAS, D. & BURNSTEIN, Y. (1984). Isolation and partial purification of a clonidine-displacing endogenous brain substance. *Eur. J. Biochem.*, **172,** 131–145.

BIRMINGHAM, M.K., SAR, M. & STUMPF, W.E. (1993). Dexamethasone target sites in the central nervous system and their potential relevance to mental illness. *Cell. Mol. Neurobiol.*, **13,** 373–386.

BRICCA, G., DONTENWILL, M., MOLINES, A., FELDMAN, J., BELCOURT, A. & BOUSQUET, P. (1989). The imidazoline preferring receptor: binding studies in bovine, rat and human brainstem. *Eur. J. Pharmacol.*, **162,** 1–9.

BROWN, C.M., MACKINNON, A.C., MCGRATH, J.C., SPEDDING, M. & KILPATRICK, A.T. (1990). α_2-Adrenoceptor subtypes and imidazoline-like binding sites in the rat brain. *Br. J. Pharmacol.*, **99,** 803–809.

BROWN, C.M., MACKINNON, A.C., REDFERN, W.S., HICKS, P.E., KILPATRICK, A.T., SMALL, C., CLAGUE, R.U., CLARK, R., MACFARLAGE, C.B. & SPEDDING, M. (1993). The pharmacology of RS-15385-197, a potent and selective α_2-adrenoceptor antagonist. *Br. J. Pharmacol.*, **108,** 516–525.

BROWN, C.M., MACKINNON, A.C., REDFERN, W.S., WILLIAMS, A., LINTON, C., STEWART, M., CLAGUE, R.U., CLARK, R. & SPEDDING, M. (1995). RS-45041-190, a selective, high-affinity ligand for I_2 imidazoline receptors. *Br. J. Pharmacol.*, **116,** 1737–1744.

CHENG, Y.C. & PRUSOFF, W.H. (1973). Relationship between the inhibition constant (Ki) and the concentration of inhibitor which causes 50 percent inhibition (I_{50}) of an enzymic reaction. *Biochem. Pharmacol.*, **22,** 3099–3108.

CHRONWALL, B.M. (1985). Anatomy and physiology of the neuroendocrine arcuate nucleus. *Peptides*, **6** suppl. 2, 1–11

COUPRY, I., ATLAS, D., PODEVIN, R., UZIELLI, I. & PARINI, A. (1989). Imidazoline-guanidinium receptive sites in renal proximal tubule: asymmetric distribution, regulation by cations and interaction with an endogenous clonidine displacing substance. *J. Pharmacol. Exp. Ther.*, **252,** 293–299.

ERNSBERGER, P. (1992). Heterogeneity of imidazoline binding sites: proposed I_1 and I_2 subtypes. *Fundam. Clin. Pharmacol.*, **6,** 18P.

ERNSBERGER, P., MEELEY, M.P., MANN, J.J. & REIS, D.J. (1987). Clonidine binds to imidazole binding sites as well as α_2-adrenoceptors in the ventrolateral medulla. *Eur. J. Pharmacol.*, **134,** 1–13.

GEHLERT, D.R., GACKENHEIMER, S.L. & SCHOBER, D.A. (1991). Autoradiographic localization of subtypes of angiotensin II antagonist binding in the rat brain. *Neuroscience*, **44,** 501–514.

GLOVER, V., HALKET, J., WATKINS, P.J., CLOW, A., GOODWIN, B.L. & SANDLER, M. (1988). Isatin: identity with the purified endogenous monoamine oxidase inhibitor tribulin. *J. Neurochem.*, **51,** 656–659.

HAMILTON, C.A., REID, J.L. & YAKABU, M.A. (1988). [^{3}H]-Yohimbine and [^{3}H]-idazoxan bind to different sites on rabbit forebrain and kidney membranes. *Eur. J. Pharmacol.*, **146,** 345–348.

KATAOKA, K., NAKAMURA, V. & HASSLER, R. (1973). Habenulo-interpeduncular tract: a possible cholinergic neuron in rat brain. *Brain Res.*, **62,** 264–267.

LANIER, S.M., IVKOVIC, B., SINGH, I., NEUMEYER, J.L. & BAKTHAVACHALAM, V. (1993). Visualization of multiple imidazoline/guanidium-receptive sites. *J. Biol. Chem.*, **268,** 16047-16051.

LI, G., REGUNATHAN, S., BARROW, C.J., ESHRAGHI, J., COOPER, R. & REIS, D.J. (1994). Agmatine: an endogenous clonidine-displacing substance in the brain. *Science*, **263,** 966–969.

LIONE, L.A., NUTT, D.J., LEWIS, J., HUNTER, J. & TOWERS, P. (1995). [^{3}H]2-(2-benzo-furanyl)2-imidazoline: a new radioligand for the study of rabbit brain non-adrenoceptor idazoxan binding sites (I_2-sites). *Br. J. Pharmacol.*, **114,** 412P.

MACKINNON, A.C., BROWN, C.M., SPEDDING, M. & KILPATRICK, A.T. (1989). [^{3}H]-Idazoxan binds with high affinity to two sites on hamster adipocytes: an α_2-adrenoceptor and a non-adrenoceptor site. *Br. J. Pharmacol.*, **98,** 1143–1150.

MACKINNON, A.C., BROWN, C.M., STEWART, M. & SPEDDING, M. (1993). [^{3}H]-*p*-aminoclonidine and [^{3}H]-idazoxan label different populations of imidazoline sites on rat kidney. *Eur. J. Pharmacol.*, **232,** 79–87.

MACKINNON, A.C., PARNES, H. & BROWN, C.M. (1995). [^{3}H]-RS-45041-190: a potent and selective radioligand for I_2 imidazoline receptors. *Br. J. Pharmacol.*, **115,** 32P.

MACKINNON, A.C., STEWART, M., SPEDDING, M. & BROWN, C.M. (1992). Autoradiographic distribution of imidazoline sites in rat brain labelled by [^{3}H]-idazoxan and potential endogenous ligands. *Fundam. Clin. Pharmacol.*, **6,** (Suppl 1), 45s.

MALLARD, N.J., HUDSON, A.L. & NUTT, D.J. (1992). Characterization and autoradiographical localization of non-adrenoceptor idazoxan binding sites in the rat brain. *Br. J. Pharmacol.*, **106,** 1018–1027.

MUNSON, P.J. & RODBARD, D. (1980). A versatile computerised approach for characterization of ligand binding systems. *Anal. Biochem.*, **107,** 220–239.

OLMOS, G., GABILONDO, A.M., MIRALLES, A., ESCRIBA, P.V. & GARCIA-SEVILLA, J.A. (1993). Chronic treatment with the monoamine oxidase inhibitors clorgyline and pargyline down-regulates non-adrenoceptor [^{3}H]-idazoxan binding sites in the rat brain. *Br. J. Pharmacol.*, **108,** 597–603.

PAXINOS, G. & WATSON, D. (1986). *The Rat Brain in Stereotaxic Coordinates.* New York: Academic Press.

ROSAS-ARRELANO, M.P., SOLANO-FLORES, L.P. & CIRIELLO, J. (1993). Effect of arcuate nucleus activation on neuronal activity in subfornical organ. *Brain Res.*, **619,** 352–356.

SAURA, J., KETTLER, R., DA PRADA, M. & RICHARDS, J.G. (1992). Quantitative enzyme radioautography with [^{3}H]-Ro 41-1049 and [^{3}H]-Ro 19-6327 in vitro: localization and abundance of MAO-A and MAO-B in rat CNS, peripheral organs and human brains. *J. Neurosci.*, **12,** 1977–1999.

SIM, L.J. & JOSEPH, S.A. (1991). Arcuate nucleus projections to brainstem regions which modulate nociception. *J. Chem. Neuroanat.*, **4,** 97–109.

SONG, K., ALLEN, A.M., PAXINOS, G. & MENDELSOHN, F.A. (1992). Mapping of angiotensin II receptor subtype heterogeneity in rat brain. *J. Comp. Neurol.*, **316,** 467–484.

YABLONSKY, F. & DAUSSE, J.P. (1989). Amiloride interacts with [^{3}H]-idazoxan and [^{3}H]-rauwolscine binding sites in rabbit urethra. *Eur. J. Pharmacol.*, **164,** 167–170.

ZAMIR, N., PALKOVITS, M. & BROWNSTEIN, M. (1985). Distribution of immunoreactive Met-enkephalin-Arg6-Gly7-Leu8 and Leu-enkephalin in discrete regions of the rat brain. *Brain Res.*, **326,** 1–8.

(Received March 8, 1995
Revised May 26, 1995
Accepted June 1, 1995)